INFLUENCE OF HUMAN BODY SHAPE AND POSING ON EMF EXPOSURE

**A. Cortel[1], N. Varsier[1], V. Dronne[1], O. Colas[1], M. F. Wong[1], E. Nicolas[2], F. Jacquin[2] and J. Wiart[1]**

*[1] France Télécom R&D – RESA/FACE 38-40, rue du Général Leclerc - 92794 Issy Moulineaux.*
*email : {albert.cortelcarrasco ; nadege.varsier ; olivier2.colas ; manfai.wong ; joe.wiart}@.francetelecom.com*
*[2] Télédiffusion de France, 75732 Paris cedex 15, France*
*email : {emmanuel.nicolas ; francois.jacquin}@tdf.fr*

## ABSTRACT

ICNIRP guidelines have defined basic restrictions in terms of SAR (Specific Absorption Rate) and reference levels in terms of field strength to protect public and workers from the exposure to electromagnetic fields (EMF). The compliance to the field limit implies the compliance to the SAR limit assuming a given a transfer function between an incident wave and the power absorption in a human body. This relation depends on the frequency but also on the body shape. The aim of this study is to analyze the influence of human body shape and posing on the local and whole body SAR.

## I. INTRODUCTION

Electromagnetic safety guidelines [1, 2] such as those of ICNIRP[1] have defined basic restrictions in terms of SAR (Specific Absorption Rate) and reference levels in terms of field strength to protect public and workers from the exposure to electromagnetic fields (EMF). The compliance to the field limit implies the compliance to the SAR limit. However the non-compliance to the field limit does not mean necessarily non compliance to the basic restrictions. The reference levels offer a simpler way for assessing compliance and generally the limits are more stringent, i.e. some margins on the field strength may exist before the fundamental SAR limit is reached. However a margin assessed for a given human body shape may be different for another one. The absorption of electromagnetic waves depends on the morphology. As well, the posing has an influence, standing or sitting matters for the absorption. It is also well known that standing on a perfectly conducting ground plane doubles the height of the body by the theory of images.

The aim of this study is to analyze the influence of human body shape and posing on the local and whole body SAR. The analysis is carried out through FDTD (Finite Difference Time Domain) [3] simulations using different scaled models of human body and sources at different frequencies. The SAR for the different configurations have been calculated and normalized to the incident field. Thus, for each configuration maximum field strength can be deduced in order to comply with the SAR limit. The relative variation is studied between the configurations for both the whole body SAR as well as the local SAR.

## II. INFLUENCE OF BODY SHAPE

### II.1. Methodology

The human body model is the Zubal phantom from Yale University [4]. Regarding body shape, from this reference model, 9 models have been derived with different heights and weights by using statistical data available on human height (Tab. 1) and body mass index (BMI) (Tab. 2). The BMI is a measure of human shape; it is defined by the formula:

$$BMI(kg/m^2) = \frac{weight(kg)}{height(m)^2} \quad (1)$$

3 weights are derived from BMI statistics (Tab. 2) by discarding the lower and upper 5 %, thus minimum, maximum and mean values of BMI are obtained (Tab. 3). 3 heights are chosen according to mean value, minimum and maximum are given by the mean minus or plus 2 standard deviations. The 9 models characteristics are given in Tab. 4. They are scaled from the original Zubal phantom. The 9 models have then been exposed to plane waves from face and side and an array of 2 dipoles at different distances (Fig. 1). The simulations are carried out at 100 MHz.

Tab. 1. Human body height statistics

| Height (cm) - men | | Height (cm) – women | |
|---|---|---|---|
| Mean | Standard deviation | Mean | Standard deviation |
| 174,1 | 7,1 | 161,9 | 6,5 |

*Source : "Enquête permanente sur les conditions de vie", France, Insee, Mai 2001*

Tab. 2. Population distribution according to BMI

| | BMI (%) | | | | | | |
|---|---|---|---|---|---|---|---|
| | <18 | [18-20[ | [20-25[ | [25-27[ | [27-30[ | 30+ | ***mean*** |
| Men | 0,7 | 3,3 | 45,1 | 21,7 | 18,1 | 11,1 | ***25,4*** |
| Women | 3,1 | 11,5 | 47,4 | 12,6 | 13,1 | 12,2 | ***24,4*** |

*Source : "Enquête de santé par interview", Institut Scientifique de la Santé Publique, Belgique, 2001*

Tab. 3. Minimum, maximum and mean values of BMI

| | *BMI (kg/m²)* |
|---|---|
| Minimum | 19,13 |
| Mean | 25 |
| Maximum | 33,22 |

Tab. 4. Height and weight of the 9 phantom models

| Model ID | Height (m) | Weigtht (kg) |
|---|---|---|
| 11 | | 48,85 |
| 12 | 1,598 | 63,84 |
| 13 | | 84,84 |
| 21 | | 57,98 |
| 22 | 1,741 | 75,77 |
| 23 | | 100,70 |
| 31 | | 67,76 |
| 32 | 1,882 | 88,55 |
| 33 | | 117,67 |

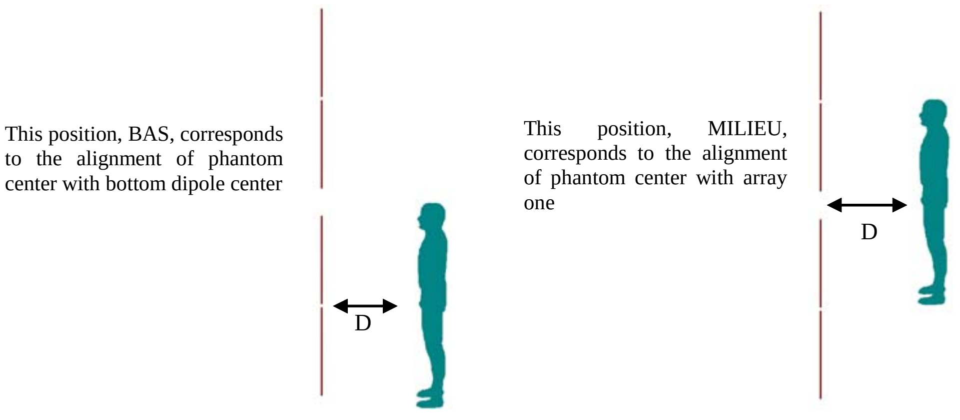


Fig. 1. 2 dipoles array exposures

### II.2. Results

The results are computed using FDTD with the help of a Huygens box for the incident field either a plane wave or the near field radiated by the dipole array. The SAR is evaluated for whole body and localized peak values. The SAR is proportional to the power flux density. Thus we can define a maximum ambient field such that the limit in terms SAR, whole body or local peak, is reached:

$$E_{\max\lim it} = \sqrt{\frac{SAR_{\lim ite}}{SAR}} E_{ambient} \quad (2)$$

where SAR is given with respect to $E_{ambient}$, which is chosen as the root of the quadratic mean of the electric field strength over the Huygens box. Fig. 2 and Fig. 3 show the maximum ambient field with respect to the weight for compliance with whole body SAR and local peak SAR respectively. It is interesting to compare this maximum ambient field with the reference level which is 61 V/m at 100 MHz. As expected, while-body SAR varies smoothly with respect to weight:

- the maximum ambient field to fulfill the limit has a big extent, up to 50 V/m difference depending on the weight,
- most restrictive found here is an incident plane-wave on the side,
- local peak SAR is less smooth with respect to weight.

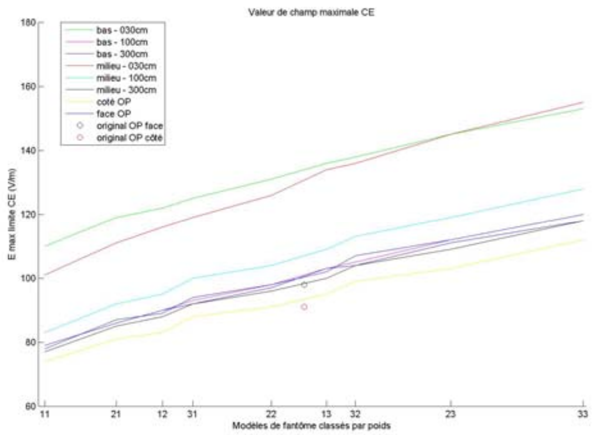


Fig. 2. Maximum E field strength to fulfill whole body SAR

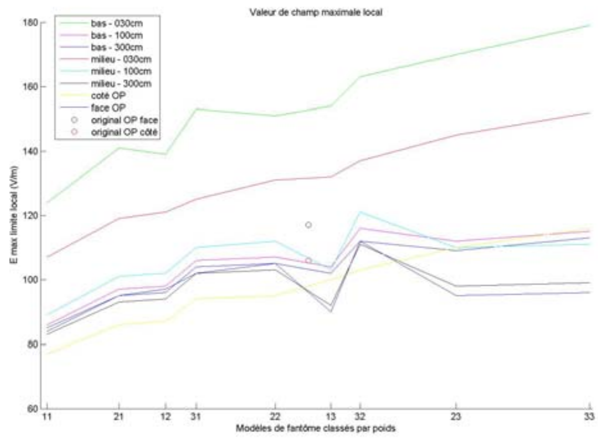


Fig. 3. Maximum ambient E fied strength to fulfill local SAR

## IV. INFLUENCE OF FAT

Whereas a uniform transformation of the Zubal phantom has been carried out, further studies include a closer look into the role of fat in this morphology deformation. For this purpose, 7 models are constructed by non-uniformly adding layers of fat: zub_gras#1_#2 means that #1 additional layer(s) is(are) added to the phantom on the surface of the body and #2 layer(s) is(are) added around the abdomen. The weights vary from 87 kg to 91 kg. Fig. 4 and Fig. 5 show the variations of maximum ambient field for compliance to whole-body SAR and peak local SAR respectively, when the phantoms are exposed to plane waves from side and face directions at 100, 200, 464, 900 and 2100 MHz. The maximum relative variation is less than 5 % for both whole-body SAR and peak local SAR.

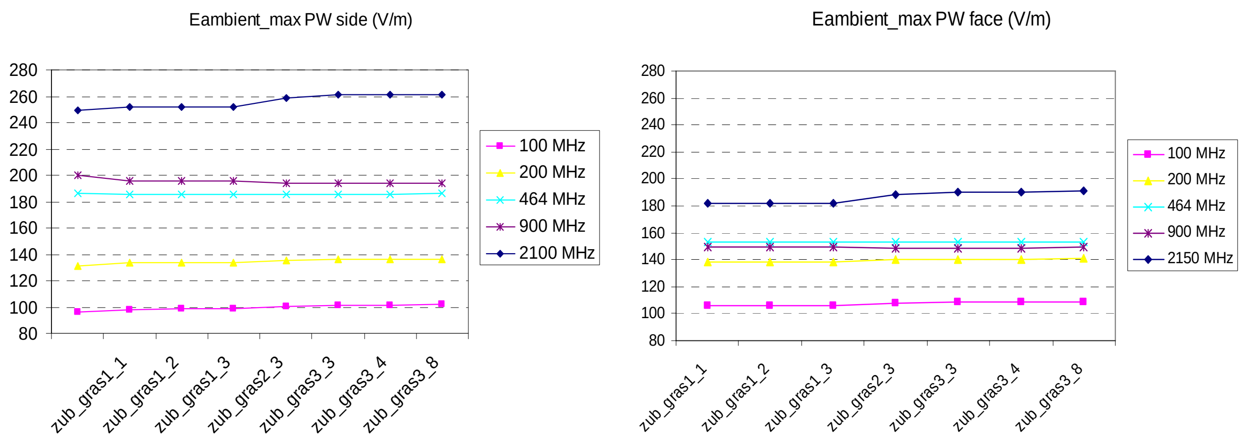


Fig. 4. Variation of maximum ambient field to fulfil whole body SAR for plane wave exposures from side (left) and face (right)

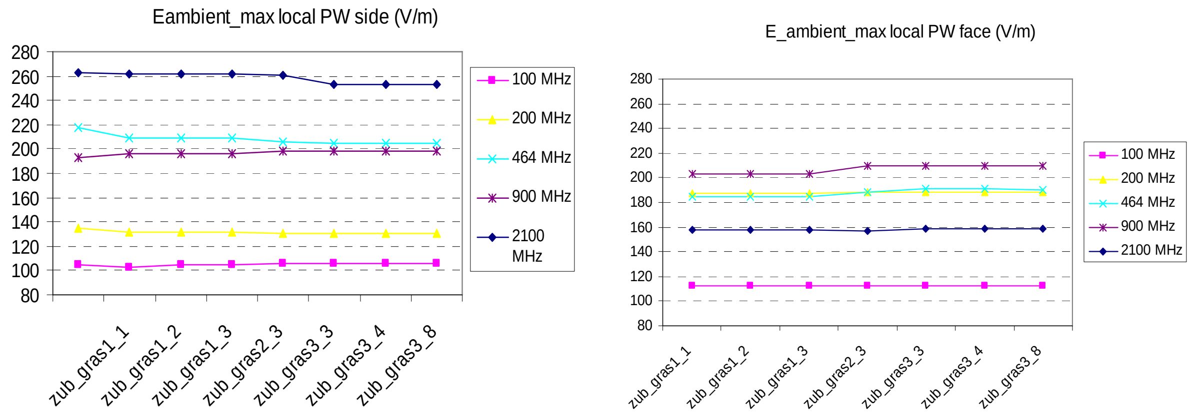


Fig. 5. Variation of maximum ambient field to fulfil peak local SAR for plane wave exposures from side (left) and face (right)

## V. PHANTOM FOR POSING

Regarding posing, the challenge is to deform the segmented phantom. Each body part of the phantom is identified using labelling. This method allows to manage one body part without interacting with another. Then each labelled body part can be rotated using a typical rotation matrix. And using an image fitting technique we are able to reconstruct our initial phantom 3D image in different positions like sitting (Fig. 6).

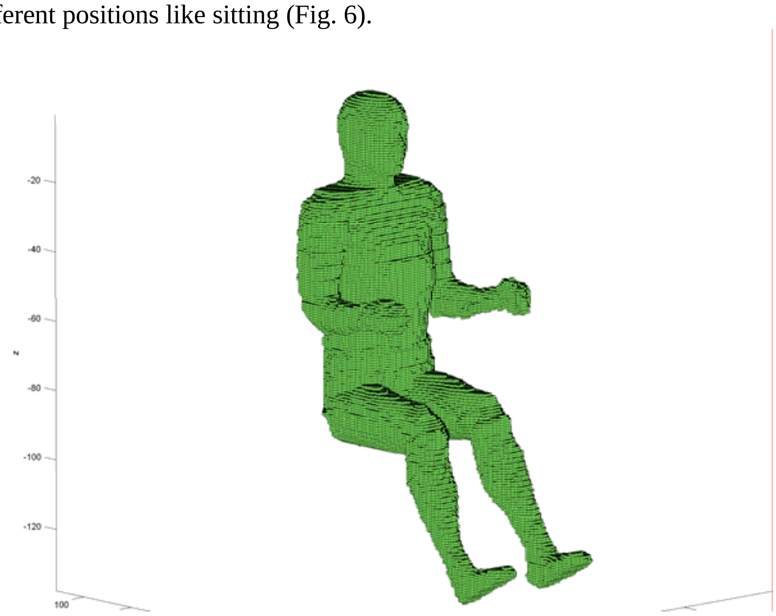

Fig. 6. Zubal phantom deformed to sitting position

## REFERENCES


[1] "Guidelines for limiting exposure to time-varying electric, magnetic, and electromagnetic fields (up to 300 GHz)," *Health Physics*, vol. 74, 1998.

[2] "Safety levels with respect to human exposure to radiofrequency electromagnetic fields, 3 kHz to 30 GHz," *IEEE standard C95.1*, 1999.

[3] A. Taflove, *Computational Electrodynamics. The Finite Difference Time Domain Method.* Boston: Artech House, 1995.

[4] I. G. Zubal, C. R. Harrell, E. O. Smith, Z. Rattner, G. Gindi, and P. B. Hoffer, "Computerized 3D segmented humain anatomy," *Med. Phys.*, vol. 21, pp. 299-302, 1994.